

Local electronic structure of Fe²⁺ impurities in MgO thin films: Temperature dependent soft x-ray absorption spectroscopy study

T. Haupricht,¹ R. Sutarto,^{1,*} M. W. Haverkort,^{1,†} H. Ott,^{1,‡} A. Tanaka,²
H. H. Hsieh,³ H.-J. Lin,⁴ C. T. Chen,⁴ Z. Hu,⁵ and L. H. Tjeng⁵

¹*II. Physikalisches Institut, Universität zu Köln, Zùlpicher Str. 77, 50937 Köln, Germany*

²*Department of Quantum Matter, ADSM, Hiroshima University, Higashi-Hiroshima 739-8530, Japan*

³*Chung Cheng Institute of Technology, National Defense University, Taoyuan 335, Taiwan*

⁴*National Synchrotron Radiation Research Center (NSRRC), 101 Hsin-Ann Road, Hsinchu 30077, Taiwan*

⁵*Max Planck Institute for Chemical Physics of Solids, Nöthnitzerstr. 40, 01187 Dresden, Germany*

(Dated: February 24, 2024)

We report on the local electronic structure of Fe impurities in MgO thin films. Using soft x-ray absorption spectroscopy (XAS) we verified that the Fe impurities are all in the 2+ valence state. The fine details in the line shape of the Fe $L_{2,3}$ edges provide direct evidence for the presence of a dynamical Jahn-Teller distortion. We are able to determine the magnitude of the effective D_{4h} crystal field energies. We also observed a strong temperature dependence in the spectra which we can attribute to the thermal population of low-lying excited states that are present due to the spin-orbit coupling in the Fe $3d$. Using this Fe²⁺ impurity system as an example, we show that an accurate measurement of the orbital moment in Fe₃O₄ will provide a direct estimate for the effective local low-symmetry crystal fields on the Fe²⁺ sites, important for the theoretical modeling of the formation of orbital ordering.

PACS numbers: 71.70.Ch, 71.70.Ej, 75.10.Dg, 78.70.Dm

Magnetite is one of the most controversially discussed systems in solid state physics.¹ It shows a first order anomaly in the temperature dependence of the electrical conductivity at 120 K, i.e., the famous Verwey transition² which is accompanied by a structural phase transition from the cubic inverse spinel to a distorted structure. It is only very recently that one realizes that this transition may involve not only charge ordering of Fe²⁺ and Fe³⁺ ions but also t_{2g} orbital ordering at the Fe²⁺ sites.³⁻⁵ Important in this regard are the recent results from band theory studies^{6,7} in which the charge and orbital occupations were calculated based on the available crystal structure data.^{3,4}

It is highly desired to determine experimentally the electronic structure of Fe₃O₄ and especially the local energetics of the Fe²⁺ sites in order to test the conditions under which the t_{2g} orbital polarization and ordering can occur. Unfortunately, a direct approach to this system is difficult since the simultaneous presence of Fe²⁺ and Fe³⁺ valences as well as octahedral and tetrahedral sites makes standard electron spectroscopic methods to yield rather broad spectral line shapes, i.e., too featureless for a precise analysis concerning the details about the effective crystal fields with a symmetry lower than O_h .⁸

Here we report on our study of the electronic structure of Fe impurities in MgO thin films. Having the local quasi-octahedral (O_h) symmetry and similar metal-oxygen bond lengths, the impurity system could serve as a valuable reference for the more complex Fe²⁺ containing magnetite. Using soft x-ray absorption spectroscopy (XAS) and an analysis based on full multiplet cluster calculations we found that the Fe impurities are all in the 2+ charge state and that a dynamical Jahn-Teller distortion is clearly present. The spectra showed a strong

temperature dependence which can be traced back to the existence of low-lying excited states due to the presence of the spin-orbit interaction. We were able to make estimates concerning the magnitude and temperature dependence of the orbital and spin contributions to the local magnetic moments. We infer that these local effects need to be included when interpreting the temperature dependence of the orbital and spin moments in magnetite across the Verwey transition.

Fe_xMg_{1-x}O samples were prepared as polycrystalline thin films in an ultra-high vacuum molecular beam epitaxy (MBE) system with a base pressure of 5×10^{-10} mbar. High purity Mg and Fe metal were co-evaporated from alumina crucibles onto clean Cu substrates. Molecular oxygen was simultaneously supplied through a leak valve. The oxygen partial pressure was kept at about 1×10^{-7} mbar and monitored by a quadrupole mass spectrometer during growth. The Mg effusion cell temperature was kept at 315 °C corresponding to a Mg deposition rate of 2.6 Å/min as verified using a quartz crystal thickness monitor. During growth the substrate temperature was kept at 250 °C which led to a distillation process that allows the growth of stoichiometric MgO. This resulted in a MgO deposition rate of about 4 Å/min. The thickness of the Fe_xMg_{1-x}O films was about 120 Å. The use of thin films on metallic substrates was necessary to avoid charging problems which otherwise readily occur in electron spectroscopic experiments on bulk insulators like MgO. Clean Cu substrates were prepared by growing roughly 1000 Å thick Cu films *in-situ* on top of atomically-flat, epi-polished and oxygen-annealed MgO substrates.

The XAS measurements were performed at the 11A Dragon beamline of the National Synchrotron Radiation

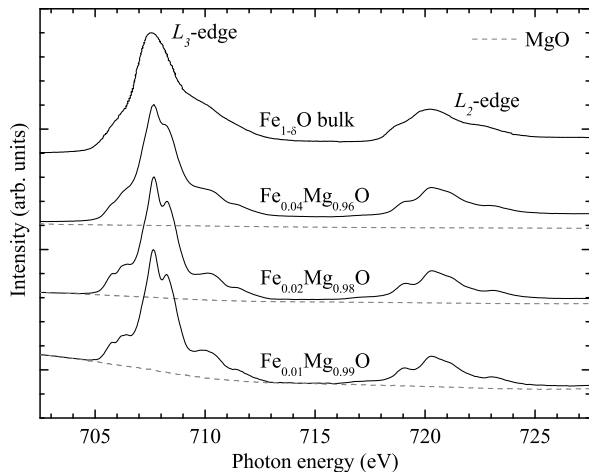


FIG. 1. Fe $L_{2,3}$ XAS spectra of $\text{Fe}_x\text{Mg}_{1-x}\text{O}$ films for $x = 0.04, 0.02, 0.01$. Included is also the spectrum of bulk $\text{Fe}_{1-\delta}\text{O}$ (top curve, reproduced from Ref. 11). The underlying dashed lines represent the XAS signal of a pure MgO film in the photon energy region of the Fe $L_{2,3}$, scaled to fit the pre-edge background of the respective $\text{Fe}_x\text{Mg}_{1-x}\text{O}$ spectrum. All spectra were taken at room temperature.

Research Center (NSRRC) in Taiwan.^{9,10} The photon energy resolution at the Fe $L_{2,3}$ edges ($h\nu \approx 700\text{--}730$ eV) was set at about 0.35 eV. The spectra were recorded using the total electron yield (TEY) method in the normal light incidence. The base pressure of the XAS chamber was 2×10^{-10} mbar. The MBE system was directly connected to this XAS chamber so that the freshly prepared samples could be transferred and measured all *in-vacuo*, thereby assuring the cleanliness and reliability of the spectra presented here.

In Fig. 1 we show the experimental Fe $L_{2,3}$ XAS spectra of $\text{Fe}_x\text{Mg}_{1-x}\text{O}$ films for $x = 0.04, 0.02$, and 0.01 . We have also included the spectra of a bulk $\text{Fe}_{1-\delta}\text{O}$ crystal (reproduced from Ref. 11) and of a pure MgO film (underlying dashed lines) as references. The MgO spectra have been scaled to fit the pre-edge background of the respective $\text{Fe}_x\text{Mg}_{1-x}\text{O}$ spectrum. The pure MgO film was prepared under the same conditions as the $\text{Fe}_x\text{Mg}_{1-x}\text{O}$ samples, i.e., it has $x = 0.00$. The Fe $L_{2,3}$ spectra are dominated by the Fe $2p$ core-hole spin-orbit coupling, which splits the spectrum roughly into two parts, namely the L_3 ($h\nu \approx 708$ eV) and L_2 ($h\nu \approx 721$ eV) white line regions. The line shapes of the spectra depend strongly on the multiplet structure given by the atomic-like Fe $2p\text{--}3d$ and $3d\text{--}3d$ Coulomb and exchange interactions, as well as by the surrounding solid.

In going from bulk $\text{Fe}_{1-\delta}\text{O}$ to the films with decreasing Fe concentrations, we can clearly observe that the spectral features become sharper. This can be taken as an indication for the presence of inter-Fe interactions in the more concentrated systems. Here we would like to note that the presence of Fe^{3+} species may also contribute to the broad spectral features of bulk $\text{Fe}_{1-\delta}\text{O}$, a mate-

rial known to have inherent defects.^{12,13} For Fe concentrations lower than 2% the spectra do not significantly change anymore - apparently here we already arrived at the impurity limit. We notice that for the lowest Fe concentrations the pre-edge XAS background is increasing. This can be attributed to the contribution of the MgO to the XAS signal in the Fe $L_{2,3}$ region as shown by the spectrum of the pure MgO film.

We now focus on the temperature dependence of the spectra. Fig. 2 shows a close-up of the experimental Fe L_3 and L_2 XAS spectra of $\text{Fe}_{0.02}\text{Mg}_{0.98}\text{O}$ for various temperatures ranging from 77 up to 500 K. For clarity, we here subtracted the XAS background coming from the pure MgO film in the Fe $L_{2,3}$ region. Clear and systematic changes with temperature can be observed in the spectra. This can be taken as a direct indication for the presence of local low-lying excited states.

To interpret and understand the spectra and their temperature dependence, we have performed simulations of the atomic-like $2p^63d^n \rightarrow 2p^53d^{n+1}$ ($n = 6$ for Fe^{2+}) transitions using the well-proven configuration-interaction cluster model.^{14–16} Within this method we have treated the Fe impurity site as an FeO_6 cluster which includes the full atomic multiplet theory and the local effects of the solid. It accounts for the intra-atomic $3d\text{--}3d$ and $2p\text{--}3d$ Coulomb interactions, the atomic $2p$ and $3d$ spin-orbit couplings, the local crystal field, and the O $2p\text{--}Fe$ $3d$ hybridization. This hybridization is taken into account by adding the $3d^{n+1}\underline{L}$ and $3d^{n+2}\underline{L}^2$ etc. states to the starting $3d^n$ configuration, where \underline{L} denotes a hole in the O p ligands. Parameters for the multipole part of the Coulomb interactions were given by the Hartree-Fock values,¹⁴ while the monopole parts (U_{dd} , U_{pd}) were estimated from photoemission experiments on FeO .¹⁷ The one-electron parameters such as the O $2p\text{--}Fe$ $3d$ charge-transfer energies and integrals as well as the crystal field values were tuned to find the best match to the experimental spectra. The simulations were carried out using the program XTLS 8.3.^{14,18}

Starting with the simple crystal field scheme, an Fe ion in the O_h coordination will have its $3d$ states split into the lower lying t_{2g} and higher e_g levels, with the splitting given by 10Dq of order 1 eV (see Fig. 3). For an Fe^{2+} ion, 5 electrons will occupy all the available spin-up states. The remaining electron occupies one of the three spin-down t_{2g} orbitals ($t_{2g}^4e_g^2$), giving the high spin $S = 2$ Hund's rule ground state. In a multiplet scheme, neglecting the spin-orbit interaction, the ground state is termed the $^5T_{2g}$ state, well separated by about 1 eV or more from the higher lying 5E_g and other lower spin configurations. Assigning a pseudo orbital momentum of $\tilde{L} = 1$ to the open t_{2g} shell,^{19,20} the spin-orbit interaction will couple it to the $S = 2$ spin, resulting in three different states with $\tilde{J} = 1, 2$, and 3 . The presence of the spin-orbit coupling in the $3d$ shell thus splits the 15-fold $^5T_{2g}$ state into the \tilde{J} states with degeneracies of 3, 5, and 7, respectively (see Fig. 3). Using typical parameters for FeO ,^{14,18} we find an energy separation between them of about 33 meV

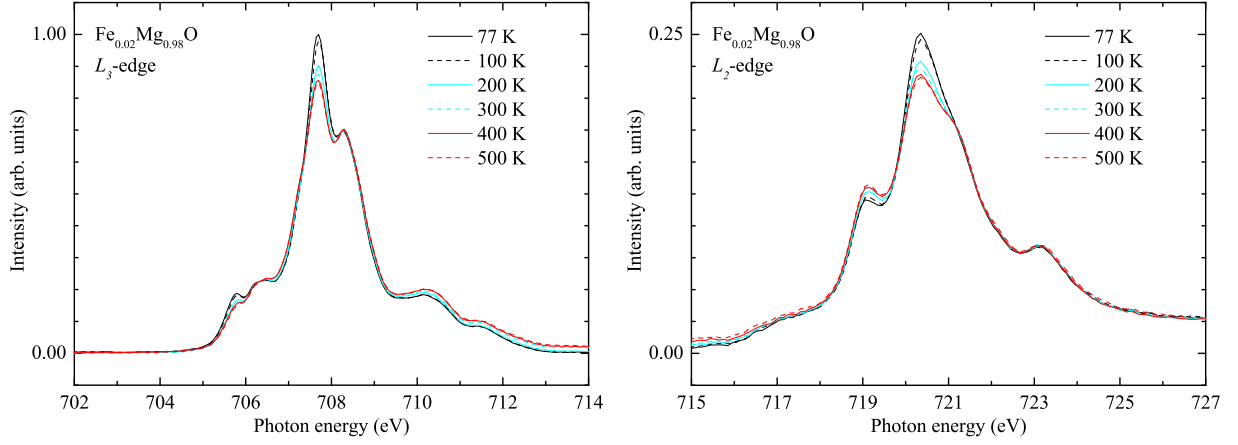


FIG. 2. (Color online) Temperature dependence of the experimental Fe L_3 and L_2 XAS spectra of $\text{Fe}_{0.02}\text{Mg}_{0.98}\text{O}$ after subtraction of the pure MgO film background.

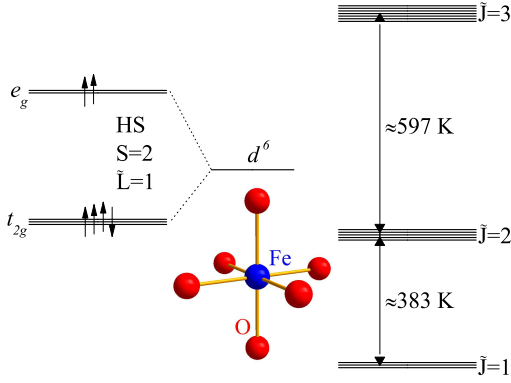


FIG. 3. (Color online) Energy level diagrams for a Fe^{2+} cluster in the O_h coordination in a crystal field (left) and a full multiplet (right) scheme. HS denotes the Hund's rule high spin configuration

($\simeq 383$ K) and 51 meV ($\simeq 597$ K), respectively.

Important for the understanding of the line shape of the Fe $L_{2,3}$ XAS spectra and their temperature dependence is that initial states with different quantum numbers could produce quite different XAS spectra, since the dipole selection rules, e.g., $\Delta J = 0, \pm 1$, will dictate which of the possible final states can be reached in the photo-absorption process. This is shown in Fig. 4. Indeed, each of the three different $\tilde{J} = 1, 2$, and 3 states has its own characteristic XAS spectrum. It is then also quite natural to expect a strong temperature dependence for the XAS spectrum of a Fe^{2+} system if an increase in temperature causes a thermal population of the $\tilde{J} = 2$ and 3 excited states at the expense of a depopulation of the $\tilde{J} = 1$ ground state.

Yet, a detailed comparison between the experimental spectra and the simulations for the O_h case reveals important quantitative discrepancies. A closer look is pro-

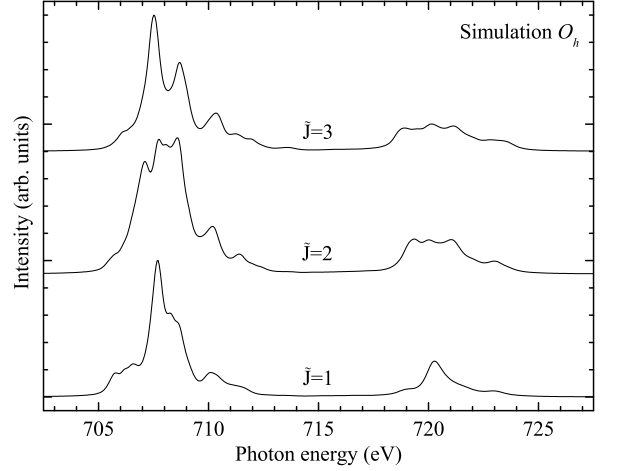


FIG. 4. Theoretical Fe $L_{2,3}$ XAS spectra starting from the three lowest multiplet states of the FeO_6 cluster in O_h symmetry, namely the $\tilde{J} = 1, 2$, and 3 manifolds of the ${}^5T_{2g}$.

vided in panel (a) of Fig. 5. One can clearly observe that neither the simulated 0 K spectrum, i.e., from the pure $\tilde{J} = 1$ ground state, nor the simulated 77 K spectrum, i.e., containing some amount of the $\tilde{J} = 2$ excited state, can reproduce the experimentally obtained 77 K spectrum. In particular, feature A is a single peak in the experiment while the O_h simulation produces two peaks, and feature B of the experiment has considerably more weight than can be generated by the simulation. All these strongly suggest that the symmetry must be lower than O_h , in line with earlier studies using optical and Mössbauer spectroscopies.^{21–25}

We have investigated two further scenarios: the D_{3d} (trigonal) and D_{4h} (tetragonal) cases. We find that the D_{3d} scenario does not provide a better fit, e.g., feature A still has a clear two peak structure and peak B has also not enough weight, as depicted in panel (c) of Fig. 5. On the other hand, we have been able to obtain a very

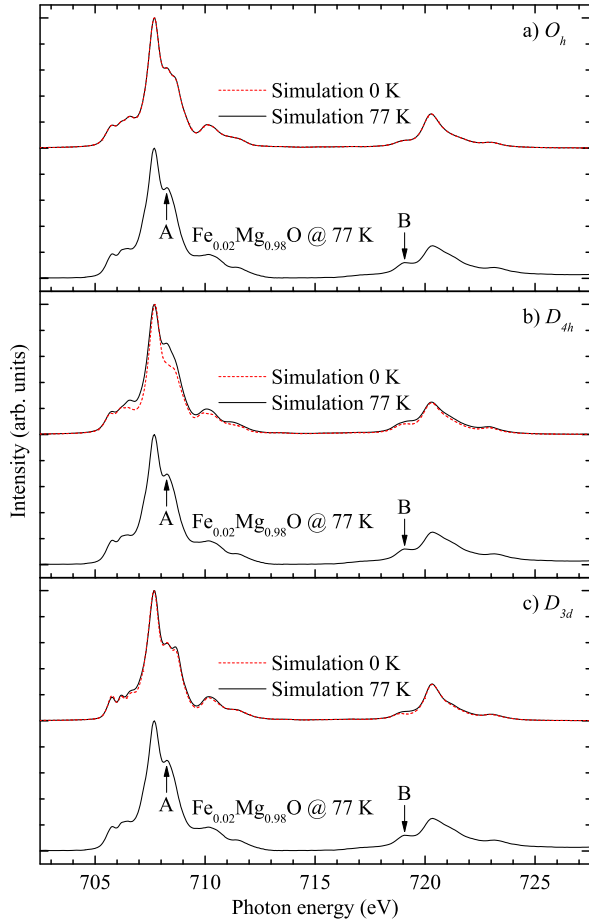


FIG. 5. (Color online) Comparison between the experimental 77 K Fe $L_{2,3}$ XAS spectrum of $\text{Fe}_{0.02}\text{Mg}_{0.98}\text{O}$ with the simulated 0 K and 77 K spectra of the FeO_6 cluster in the (a) O_h , (b) D_{4h} , and (c) D_{3d} symmetry. Parameters for the simulations are explained in the text.

good fit using the D_{4h} scenario as shown in the middle panel (b) of Fig. 5: the simulation gives more weight for peak B in better agreement with the experiment, and the simulated peak A is a more singly peak now as it is in the experiment. The overall line shape is thus well reproduced. We note that this also provides evidence that the $\text{Fe}_{0.02}\text{Mg}_{0.98}\text{O}$ film contains only Fe^{2+} ions since the simulation has been done for an FeO_6 cluster having the $3d^n$, $3d^{n+1}\underline{L}$, and $3d^{n+2}\underline{L}^2$ configurations with $n = 6$. We thus find no indication for the presence of Fe^{3+} or Fe^{1+} ions in our MBE-grown thin film samples, in contrast to other earlier studies.^{23,24,26–29}

Continuing now with the D_{4h} scenario, we also have simulated the temperature dependence of the Fe L_3 and L_2 XAS spectra. Fig. 6 shows the results. One can observe that the experimentally obtained temperature dependence (see Fig. 2) is quantitatively very well reproduced. The good agreement between simulation and experiment at all the temperatures measured can be taken as a strong indication that the D_{4h} scenario describes accurately the local symmetry of the Fe ion in MgO and

that the model parameters chosen are realistic giving also an appropriate energy separation between the ground state and the excited states. In the following we will discuss in more detail the total energy level diagram of the Fe^{2+} cluster in D_{4h} symmetry.

As already mentioned above, in O_h symmetry the Fe $3d^6$ $^5T_{2g}$ ground state is split by the spin-orbit interaction into the $\tilde{J} = 1, 2$, and 3 states. A closer look reveals that there are also smaller splittings within the $\tilde{J} = 2$ and 3 manifolds. The ground state with $\tilde{J} = 1$ is also labeled as Γ_{5g} , while the higher lying first excited states with $\tilde{J} = 2$ are given the terms Γ_{3g} and Γ_{4g} . We now switch on the D_{4h} crystal field by introducing the parameters Ds and Dt ,¹⁹ as well as differences in the O $2p$ -Fe $3d$ hopping integrals along the c -axis vs. the a -axis of the FeO_6 cluster. The D_{4h} effective crystal field parameter can then be most conveniently described as the effective energy splitting Δt_{2g} between the xy and the yz/zx states. This splitting can be determined from a total energy calculation for which the spin-orbit interaction is set to zero. Here a negative Δt_{2g} means that the xy is the lowest state (compressed octahedron). The resulting total energy diagram (including spin-orbit interaction) vs. Δt_{2g} is plotted in Fig. 7.

In going from O_h to D_{4h} with increasing Δt_{2g} , we find that the splitting between the Γ_{5g} ground state and part of the excited states Γ_{3g} and Γ_{4g} becomes reduced. It decreases from roughly 30 meV for $\Delta t_{2g} = 0$ to approximately 10 meV for $\Delta t_{2g} = -76$ meV, the value with which we find the best simulations for our XAS data. See also the inset of Fig. 7. This 10 meV value agrees very well with earlier optical and spin relaxation measurements which have inferred the existence of a state at about 100-115 cm^{-1} .^{26,27} In our simulations we need to have the splitting reduced from its large cubic value of 30 meV to this particular 10 meV number in order (1) to have sufficient admixing of the Γ_{3g} and Γ_{4g} into the primarily Γ_{5g} -like ground state so that feature A becomes more like a single peak and feature B gains substantial spectral weight as in the experiment (see Fig. 5), and (2) to obtain sufficient thermal population of the excited states with increasing temperature in the 77-500 K range so that the experimentally observed strong temperature dependence is reproduced (see Figs. 2 and 6). We would like to note that the ground state of this $3d^6$ system in the D_{4h} symmetry is a singlet, as can be seen in the inset of Fig. 7.

As indicated above, we found $\Delta t_{2g} = -76$ meV to be the optimal number for the effective energy splitting in order to achieve the best simulations for the experimental data. It is important to realize that this splitting lies well within the phonon energies of the MgO crystal.^{30,31} Therefore, rather than expecting to see a static Jahn-Teller distortion, as it is present in some Fe^{2+} containing metal complexes,^{32–34} one should take this distortion as dynamical in which the phonons are strongly coupled to the electronic degrees of freedom as pointed out by Ham and co-workers.^{22,25,35} To generate static distortions one

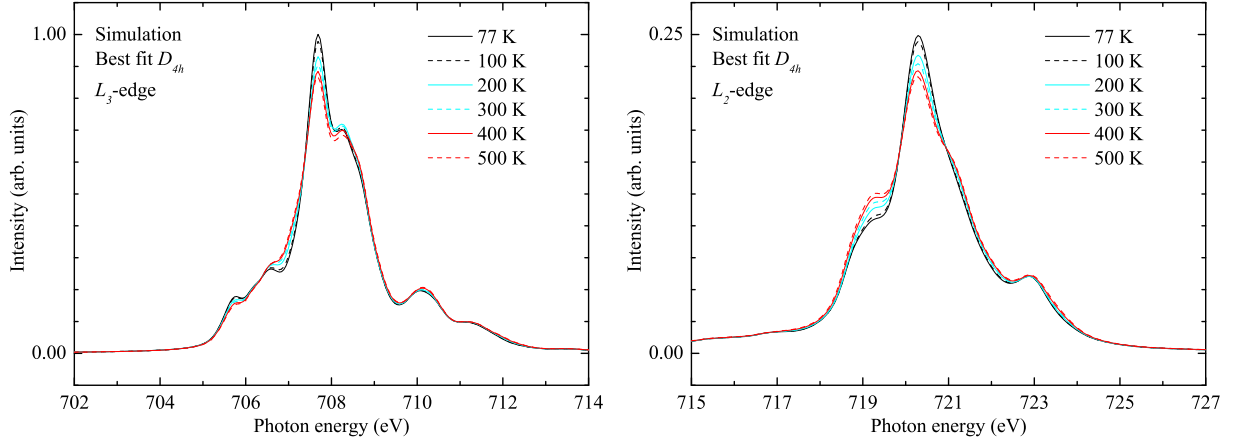


FIG. 6. (Color online) Simulations of the temperature dependence of the Fe L_3 and L_2 XAS spectra in the D_{4h} symmetry. Parameters for the simulations are explained in the text.

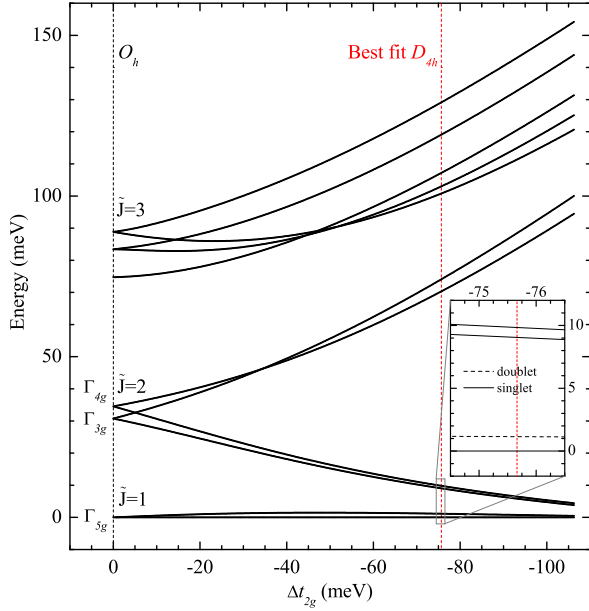


FIG. 7. (Color online) The total energy level diagram of the $\text{Fe}^{2+} \text{FeO}_6$ cluster as a function of the D_{4h} crystal field splitting expressed in terms of Δt_{2g} .

would need an effective crystal field splitting of about 0.2 eV or larger.

It is now interesting to see what consequences the presence of such a D_{4h} crystal field splitting has for the magnetic properties of the Fe^{2+} ion. We calculate the spin and orbital contributions to the magnetic moments in the presence of an exchange field (H_{ex}) of 75 meV. We chose for this value as it may be taken as a crude estimate for the case of Fe_3O_4 . Fig. 8 shows the results of the calculations for several values of the crystal field energy Δt_{2g} . For $\Delta t_{2g} = 0$, i.e., the O_h case, the orbital moment is very large, very close to $1.0 \mu_B$. Yet, it also decreases rapidly with temperature: at 500 K it becomes

$0.5 \mu_B$. This is the consequence of the thermal population of the $\tilde{J} = 2$ and 3 excited states. Upon switching on the D_{4h} crystal field to -76 meV, the orbital moment gets also reduced, to about $0.7 \mu_B$ already at 0 K. Increasing further the crystal field to -150 meV, -225 meV and -300 meV produces smaller and smaller orbital moments, i.e., about 0.4, 0.3, and $0.2 \mu_B$, respectively. The spin moment, nevertheless, always stays close to about $4 \mu_B$.

These findings could provide an interesting path to critically test recent electronic structure theories^{6,7} for the explanation of the experimentally observed complex charge and orbital order phenomena in Fe_3O_4 .³⁻⁵ An accurate measurement of the orbital moment, i.e., the orbital moment at the Fe^{2+} sites (the $\text{Fe}^{3+} 3d^5$ with their high-spin half-filled shell do not carry an orbital moment), will provide a direct estimate of the magnitude of the effective crystal field splitting. This in turn will determine whether the occupied minority t_{2g} orbital of the Fe^{2+} is made of mainly real space orbitals or has a more complex nature. Only for crystal fields substantially larger than the spin-orbit interaction one can obtain the real space orbitals necessary to build a robust orbital ordering. In this sense the measurement of $0.76 \mu_B$ orbital moment at 88 K by Huang *et al.*³⁶ would suggest the occupation of a complex t_{2g} orbital and a crystal field too small to produce a static Jahn-Teller distortion. On the other hand, the measurement by Goering *et al.*³⁷ of $0.01 \mu_B$ would support the scenario for real space orbitals and large static Jahn-Teller distortions, much more in line with the recent theoretical studies.^{6,7} Nevertheless, the issue on the magnitude of the orbital moment is not clear and is subject of debate.^{38,39}

To conclude, we have succeeded in preparing the $\text{Fe}^{2+}:\text{MgO}$ impurity system using MBE thin film technology. The resulting Fe $L_{2,3}$ soft x-ray absorption spectra display very sharp features, thereby allowing us to firmly establish that the Fe local coordination has a lower symmetry than O_h . Detailed analysis of the spectral line

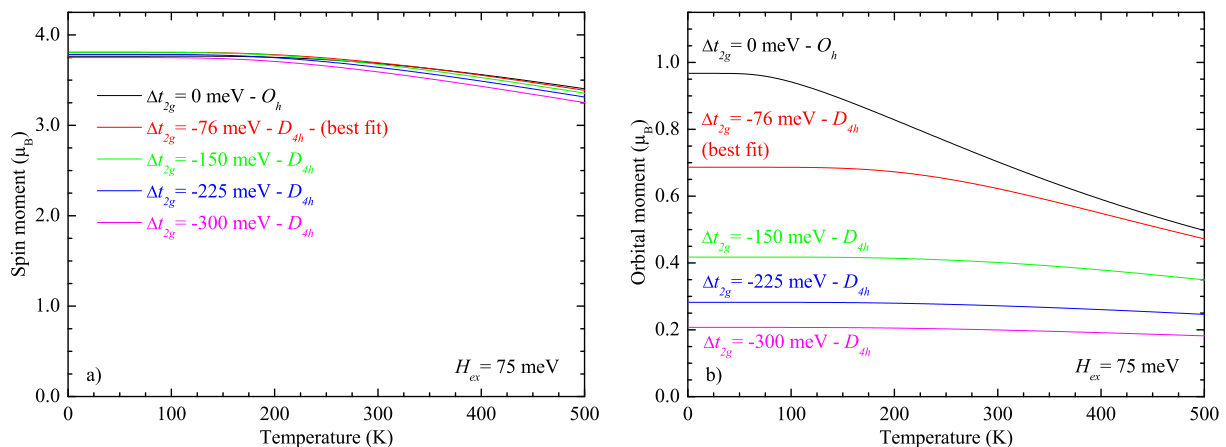


FIG. 8. (Color online) Simulated temperature dependence of the spin ($m_s = 2 \cdot S_x$, panel (a)), and orbital ($m_l = L_x$, panel (b)) contributions to the local magnetic moment of the FeO₆ cluster for various D_{4h} crystal field energies (Δt_{2g}) and an exchange field of 75 meV.

shape and its temperature dependence reveals that the local symmetry is D_{4h} with an effective t_{2g} crystal field splitting of about -76 meV. With an energy well within the phonon frequencies of MgO, this gives rise to a dynamic Jahn-Teller distortion. Using this Fe²⁺ impurity system as a model we showed that an accurate measurement of the orbital moment in Fe₃O₄ will provide a direct estimate for the effective local low-symmetry crystal fields on the Fe²⁺ sites, important for the theoretical

modeling of the formation of orbital ordering.

We gratefully acknowledge the NSRRC staff for providing us with beamtime. We would like to thank Lucie Hamdan for her skillful technical and organizational assistance in preparing the experiment. The research in Cologne is supported by the Deutsche Forschungsgemeinschaft through SFB 608. T. H. is also supported by the Bonn-Cologne Graduate School of Physics and Astronomy.

* Present address: Department of Physics and Astronomy, University of British Columbia, 6224 Agricultural Rd., Vancouver, British Columbia V6T 1Z1, Canada
† Present address: Max Planck Institute for Solid State Research, Heisenbergstr. 1, 70569 Stuttgart, Germany
‡ Present address: Shell Exploration & Production B.V., Kessler Park 1, 2288 GS Rijswijk, the Netherlands
¹ N. Tsuda, K. Nasu, A. Fujimori, and K. Siratori, *Electronic Conduction in Oxides* (Springer, New York, 2000).
² E. J. W. Verwey, *Nature*, **144**, 327 (1939).
³ J. P. Wright, J. P. Attfield, and P. G. Radaelli, *Phys. Rev. Lett.*, **87**, 266401 (2001).
⁴ J. P. Wright, J. P. Attfield, and P. G. Radaelli, *Phys. Rev. B*, **66**, 214422 (2002).
⁵ J. Schlappa, C. Schüßler-Langeheine, C. F. Chang, H. Ott, A. Tanaka, Z. Hu, M. W. Haverkort, E. Schierle, E. Weschke, G. Kaindl, and L. H. Tjeng, *Phys. Rev. Lett.*, **100**, 026406 (2008).
⁶ I. Leonov, A. N. Yaresko, V. N. Antonov, M. A. Korotin, and V. I. Anisimov, *Phys. Rev. Lett.*, **93**, 146404 (2004).
⁷ H.-T. Jeng, G. Y. Guo, and D. J. Huang, *Phys. Rev. Lett.*, **93**, 156403 (2004).
⁸ J.-H. Park, L. H. Tjeng, J. W. Allen, P. Metcalf, and C. T. Chen, *Phys. Rev. B*, **55**, 12813 (1997).
⁹ C. T. Chen and F. Sette, *Phys. Scr.*, **T31**, 119 (1990).
¹⁰ C. T. Chen and F. Sette, *Rev. Sci. Instrum.*, **60**, 1616 (1989).
¹¹ J.-H. Park, Ph.D. thesis, University of Michigan (1994).

¹² R. Jeanloz and R. M. Hazen, *Nature*, **304**, 620 (1983).
¹³ C. N. R. Rao and B. Raveau, *Transition Metal Oxides*, 2nd ed. (Wiley-VCH, 1997).
¹⁴ A. Tanaka and T. Jo, *J. Phys. Soc. Jpn.*, **63**, 2788 (1994).
¹⁵ See review by F. M. F. de Groot, *J. Electron. Spectrosc. Relat. Phenom.*, **67**, 529 (1994).
¹⁶ See review in the Theo Thole Memorial Issue, *J. Electron. Spectrosc. Relat. Phenom.*, **86**, 1 (1997).
¹⁷ A. E. Bocquet, T. Mizokawa, T. Saitoh, H. Namatame, and A. Fujimori, *Phys. Rev. B*, **46**, 3771 (1992).
¹⁸ Parameters used for the calculation of the FeO₆ cluster (in eV): $\Delta=7.5$, $U_{dd}=6.0$, $U_{cd}=7.5$, $10Dq=0.6$, $T_{pp}=0.7$, and ζ see Ref. 14, Slater integrals 75% of Hartree-Fock values.
¹⁹ C. J. Ballhausen, *Introduction to ligand field theory* (McGraw-Hill, New York, 1962).
²⁰ J. B. Goodenough, *Phys. Rev.*, **171**, 466 (1968).
²¹ G. D. Jones, *Phys. Rev.*, **155**, 259 (1967).
²² F. S. Ham, *Phys. Rev.*, **160**, 328 (1967).
²³ H. R. Leider and D. N. Pipkorn, *Phys. Rev.*, **165**, 494 (1968).
²⁴ N. B. Manson, J. T. Gourley, E. R. Vance, D. Sengupta, and G. Smith, *J. Phys. Chem. Solids*, **37**, 1145 (1976).
²⁵ A. Hjortsberg, J. T. Vallin, and F. S. Ham, *Phys. Rev. B*, **37**, 3196 (1988).
²⁶ J. Y. Wong, *Phys. Rev.*, **168**, 337 (1968).
²⁷ E. L. Wilkinson, R. L. Hartman, and J. G. Castle, *Phys. Rev.*, **171**, 299 (1968).
²⁸ J. Chappert, A. Misetich, R. B. Frankel, and N. A. Blum,

- Phys. Rev. B, **1**, 1929 (1970).
- ²⁹ F. A. Modine, E. Sonder, and R. A. Weeks, J. Appl. Phys., **48**, 3514 (1977).
- ³⁰ M. J. L. Sangster, G. Peckham, and D. H. Saunderson, J. Phys. C: Solid State Phys., **3**, 1026 (1970).
- ³¹ A. R. Oganov, M. J. Gillan, and G. D. Price, J. Chem. Phys., **118**, 10174 (2003).
- ³² B. Thole, G. van der Laan, and P. Butler, Chem. Phys. Lett., **149**, 295 (1988).
- ³³ M.-S. Liao and S. Scheiner, J. Chem. Phys., **114**, 9780 (2001).
- ³⁴ M. Bernien, J. Miguel, C. Weis, M. E. Ali, J. Kurde, B. Krumme, P. M. Panchmatia, B. Sanyal, M. Piantek, P. Srivastava, K. Baberschke, P. M. Oppeneer, O. Eriksson, W. Kuch, and H. Wende, Phys. Rev. Lett., **102**, 047202 (2009).
- ³⁵ F. S. Ham, W. M. Schwarz, and M. C. M. O'Brien, Phys. Rev., **185**, 548 (1969).
- ³⁶ D. J. Huang, C. F. Chang, H.-T. Jeng, G. Y. Guo, H.-J. Lin, W. B. Wu, H. C. Ku, A. Fujimori, Y. Takahashi, and C. T. Chen, Phys. Rev. Lett., **93**, 077204 (2004).
- ³⁷ E. Goering, S. Gold, M. Lafkioti, and G. Schütz, Europhys. Lett., **73**, 97 (2006).
- ³⁸ E. Goering, M. Lafkioti, and S. Gold, Phys. Rev. Lett., **96**, 039701 (2006).
- ³⁹ D. J. Huang, H.-J. Lin, and C. T. Chen, Phys. Rev. Lett., **96**, 039702 (2006).